Proc. Nat. Acad. Sci. USA
Vol. 72, No. 7, pp. 2606–2610, July 1975
Biochemistry

Molecular orbital studies of enzyme activity: I: Charge relay system and tetrahedral intermediate in acylation of serine proteinases*

(partial retention of diatomic differential overlap/trypsin)

STEVE SCHEINER, DANIEL A. KLEIER, AND WILLIAM N. LIPSCOMB

Gibbs Chemical Laboratory, Harvard University, Cambridge, Massachusetts 02138

Contributed by William N. Lipscomb, April 24, 1975

ABSTRACT **The charge relay system and its role in the acylation of serine proteinases is studied using the partial retention of diatomic differential overlap (PRDDO) technique to perform approximate *ab initio* molecular orbital calculations on a model of the enzyme–substrate complex. The aspartate in the charge relay system is seen to act as the ultimate proton acceptor during the charging of the serine nucleophile. A projection of the potential energy surface is obtained in a subspace corresponding to this charge transfer and to the coupled motions of active site residues and the substrate. These results together with extended basis set results for cruder models suggest that a concerted transfer of protons from Ser-195 to His-57 and from His-57 to Asp-102 occurs with an energy barrier of 20–25 kcal/mole (84–105 kJ/mole). The subsequent nucleophilic attack on the scissile peptide linkage by the charged serine is then seen to proceed energetically downhill to the tetrahedral intermediate. The formation of the tetrahedral intermediate from the Michaelis complex is calculated to be nearly thermoneutral.**

The serine proteinases [e.g., chymotrypsin (EC 3.4.21.1), trypsin (EC 3.4.21.4)] catalyze the hydrolysis of proteins during digestion in many animals and have been the subject of much research. A considerable body of evidence has accumulated which suggests that chymotrypsin-mediated hydrolysis of many substrates proceeds via the mechanism

$$E + S \underset{k_{-1}}{\overset{k_1}{\rightleftharpoons}} E{\cdot}S \xrightarrow{k_2} ES' + P_1 \xrightarrow{k_3} E + P_2 \quad [1]$$

where $E{\cdot}S$ is a Michaelis–Menten complex and ES' is an acyl enzyme intermediate (1). The acylation (step 2 in Eq. 1) is thought to pass through a tetrahedral intermediate which involves nucleophilic addition of a serine hydroxyl group to a carbonyl carbon of the substrate. There are many nonenzymatic reactions where tetrahedral intermediates of this type have been inferred (1–3). Kinetic studies (1, 4) support the existence of a tetrahedral intermediate in the acylation step of chymotrypsin and an x-ray diffraction study demonstrates that the complex formed by bovine trypsin and bovine pancreatic trypsin inhibitor (PTI) approximates a tetrahedral adduct involving a covalent bond between the carbonyl carbon of the scissile peptide linkage and the γ-oxygen of Ser-195[a] of the enzyme (5). The trypsin–PTI complex is presumed to resemble an intermediate in the productive binding of a real substrate. In general, the rate-determining step in the chymotrypsin-catalyzed hydrolysis of specific substrates is deacylation for esters and acylation for amides (1, 6). For amides, there is evidence that the rate-determining step in the formation of the acyl-enzyme complex involves the breakdown of the tetrahedral intermediate (4, 7), and studies of substituent effects on the acylation of chymotrypsin by anilides of *N*-benzoyl-L-tyrosine and *N*-acetyl-L-tyrosine (1, 8, 9) suggest that a proton transfer is involved in the transition state of the acylation step.

Recent x-ray diffraction studies of native and inhibited serine proteinases (5, 10–13) together with the kinetic studies of these enzymes and model systems (1) have led to the following proposal which elaborates the details of the acylation process. The substrate is first bound noncovalently to form a Michaelis complex, $E{\cdot}S$. In this complex the scissile peptide linkage of the substrate is near a particularly reactive nucleophile, the hydroxyl of Ser-195. The mode of attack is not firmly resolved but one plausible proposal involves a transfer of a proton from Ser-195 either to His-57 or, through the intermediacy of His-57, to Asp 102. The Ser-195 anion would then attack the carbonyl carbon of the scissile peptide linkage to form a tetrahedral intermediate. Subsequent protonation of the leaving group by His-57 followed by cleavage of the peptide linkage then yields the acyl-enzyme. A mechanism related to the one described here for serine proteinases has recently been proposed for papain (14).

In this paper we study the electronic factors responsible for the activity of the serine proteinases, using an approximate molecular orbital theory developed in this laboratory (15). This method, partial retention of diatomic differential overlap (PRDDO), has proven to be an effective method for closely reproducing minimum basis set *ab initio* results at relatively low cost. Here we apply the PRDDO method to the task of studying the charge relay system (10) of the serine proteinases and the energetics of the tetrahedral intermediate formation. We also use a more extended basis set to repeat certain key calculations in order to assess the probable error arising from the minimum basis set approximation. Our results may be compared with those obtained using a more approximate method (CNDO/2) (16).

RESULTS

In our molecular orbital calculations, the active site residues Ser-195, His-57, and Asp-102 were modeled by methanol, imidazole, and formic acid, respectively. The scissile peptide linkage was represented by a formamide molecule. The internal geometries and relative positions of the models for the residues at the active site (Fig. 1b) were obtained in the following manner. The internal geometry of imidazole was obtained from a neutron diffraction study of histidine (17). The axis between C^{γ} and the proton bonded to it in imidazole was chosen to be collinear with the C^{γ}–C^{β} axis of histidine with a bond length equal to $r(C^{\delta 2}\text{–}H^{\delta 2})$. The coordinates of $H^{\delta 1}$ were obtained from the neutron diffraction coordinates of $H^{\epsilon 2}$ by reflecting them through the plane per-

Abbreviations: PRDDO, partial retention of diatomic differential overlap; PTI, pancreatic trypsin inhibitor; I, inhibitor designation following an amino-acid number; 4-31G, a molecular orbital method; Im, imidazole; MBSE, minimum basis set errors.

* A preliminary report of this research was presented at the 4th Enzyme Mechanism Conference in San Juan, Puerto Rico, January 3, 1975.

[a] Here we use the chymotrypsin numbering system to identify the amino-acid residues.

Table 1. Proton affinities[a]

Species	Exptl.	PRDDO	4-31G[b]	MBSE[c]
Methoxide anion	408[d]	525[e]	411[e]	114
Formate anion	342[f]	473[e]	358[e]	115
Ammonia	207[g]	235[e]	222[e]	13
Imidazole	—	260[h]	—	—
Pyridine	225[i]	250[j]	—	—

[a] All energies are in kcal/mole (1 cal = 4.184 J).
[b] See Ditchfield *et al.* (25). 4-31G employs an extended basis set of Slater orbitals represented as a linear combination of gaussians.
[c] Minimum basis set error is the difference between the PRDDO proton affinity and that calculated with the 4-31G basis set.
[d] $PA(A^-) = DE(HA) - EA(A\cdot) + IP(H\cdot)$ where PA = proton affinity, DE = dissociation energy, EA = electron affinity, IP = ionization potential; $IP(H\cdot) = 313.5$ kcal/mole; $DE(CH_3O\text{-}H)$ and $EA(CH_3O\cdot)$ from ref. 26.
[e] Calculations performed using PRDDO optimized geometry.
[f] $DE(HCOO\text{-}H) - EA(HCOO\cdot)$ from ref. 21.
[g] Ref. 27.
[h] Calculations performed using geometries of Im and ImH^+ described in text.
[i] Ref. 28.
[j] Calculations performed using geometry of Bak *et al.* (29).

pendicular to the ring which contains $C^{\epsilon 1}$ and $H^{\epsilon 1}$ (see Fig. 1b). The position of this hydrogen was then optimized using the PRDDO method. The coordinates of imidazole were then transformed to superimpose on those of His-57 from Huber's x-ray structure of the complex of trypsin with pancreatic trypsin inhibitor (PTI) (12). Initial coordinates of the formate anion were those of the x-ray study for the carboxyl group of Asp-102; a proton, H_a, was placed 1.09 Å from the carbon nucleus, along the bisector of the O_{a1}–C_a–O_{a2} angle. The x-ray coordinates of Ser-195 were used to generate the coordinates of the protons of methanol. A tetrahedral methyl group was generated on C_s (see Fig. 1) with $r_{C\text{-}H} = 1.09$ Å and one of these protons, H_{s1}, placed as nearly along the C_s–C^α bond of Ser-195 as possible, i.e., within 2.5°. The position of H_o was chosen such that $r(O_s\text{–}H_o) = 0.96$ Å, $\angle C_s\text{–}O_s\text{–}H_o = 109.4°$ and the dihedral angle $\phi(N^{\epsilon 2}\text{–}C_s\text{–}O_s\text{–}H_o) = 0$. The coordinates of formamide were obtained from those of the atoms of the Lys-15I-Ala-16I linkage of the complex (I indicates residues in PTI). The H_f atom was placed along the C_f–C^α axis of Lys-15I at a distance of 1.0 Å from C_f. H_{N1} was placed along the N_f–C^α axis of Ala-16I at a distance of 1.0 Å from N_f. H_{N2} was then placed along the bisector of the larger $C_f\text{–}N_f\text{–}H_{N1}$ angle with $r(N_f\text{–}H_{N2}) = 1.0$ Å, after which its angular position was optimized. Excluding formate and imidazole from the calculations but including methanol in the position described immediately above, the formamide was allowed to pucker by synchronously bending the three substituents bonded to the carbonyl carbon, C_f, away from the central axis[b] through equal angles θ. We find that the equilibrium θ is 91° compared to 102° in the x-ray geometry.[c] The $C_f\text{–}O_f$ and $C_f\text{–}N_f$ bond lengths were optimized to 1.24 and 1.41 Å, respectively, in the nearly planar structure.

The positions of the four groups were then partially optimized in relation to one another. Including only the models of the enzyme active site residues (formate anion, neutral imidazole, and methanol) in the calculations, the imidazole was allowed two degrees of freedom. First, the imidazole was rotated about the virtual C^γ–C^β bond axis, and then about the C^α–C^β bond axis.[d] The methanol, when allowed the freedom of an axial rotation about the C_s–H_{s1} axis, was found to be already optimally oriented. The two C–O bond lengths in formate anion, $r(C_a\text{–}O_{a1})$ and $r(C_a\text{–}O_{a2})$, were optimized to 1.29 and 1.31 Å, respectively. The rotations of the imidazole ring are seen to bring $H^{\delta 1}$ into a position where its distances from the two oxygen atoms of formate differ by only 0.1 Å, in agreement with experimental findings of a bifurcated hydrogen bond between His-57 and Asp-102 (13). However, because the calculated Mulliken overlap population over atoms for the pair $H^{\delta 1}$-O_{a2} is nearly four times that of the pair $H^{\delta 1}$-O_{a1} and because O_{a1} is already hydrogen bonded to Ser-214 (13), we decided to transfer $H^{\delta 1}$ to O_{a2} during the study of the charge transfer. (See *Note Added in Proof.*)

Table 2. Mulliken group charges* during proton transfer

α	(HCOO)	$H^{\delta 1}$	$(C_3N_2H_3)$	H_o	(OCH_3)
0	−0.90	0.35	−0.36	0.25	−0.34
1/6	−0.82	0.32	−0.38	0.23	−0.35
2/6	−0.69	0.29	−0.42	0.23	−0.40
3/6	−0.55	0.26	−0.46	0.23	−0.47
4/6	−0.42	0.24	−0.49	0.25	−0.57
5/6	−0.35	0.24	−0.48	0.27	−0.67
1	−0.32	0.26	−0.46	0.30	−0.76

* Ref 23.

Two alternatives were considered for the charge transfer which activates the serine as a nucleophile. (*1*) Transfer of the seryl proton halfway to its final position on His-57 without concomitant movement of $H^{\delta 1}$ towards formate results in a calculated energy increase of 28 kcal/mole. Our PRDDO calculations show that the more likely process is (*2*) a transfer of H_o from Ser-195 to His-57 accompanied by a simultaneous transfer of $H^{\delta 1}$ to Asp-102. We feel obliged to note that any *ab initio* minimum basis set calculation will overestimate the instability of those anionic species whose negative charge is highly concentrated. Thus, methoxide and formate anions, at the minimum basis set level, should show unreasonably high proton affinities. Proton affinities for several relevant species as calculated by both the PRDDO and the extended basis set 4-31G methods are presented in Table 1. These results suggest that the PRDDO minimum basis set errors (MBSE) for deprotonation of methanol and formic acid are nearly identical. We chose α, the fractional proton transfer, as a parameter to describe a simultaneous, synchronous transfer of proton H_o from O_s to $N^{\epsilon 2}$ (a displacement of 0.7 Å) and $H^{\delta 1}$ from $N^{\delta 1}$ to O_{a2} (1.0 Å displacement) coupled with suitable C—O bond length alterations compatible with the change from formate anion to formic acid. We anticipate that the MBSE in the ΔE for charge transfer will be small since one computationally unstable anion (formate) is replaced by another (methoxide) as α varies from zero to unity. Note that $\alpha = 0$ corresponds to the arrangement H_2NCHO, CH_3OH, Im, $HCOO^-$ (Im = imidazole) in which the $N^{\delta 1}\text{–}H^{\delta 1}$ and $O_s\text{–}H_o$ distances were optimized for isolated Im and CH_3OH molecules. Since PRDDO calculations predict that this conformation is not the most stable one for the interacting total system, α is greater than zero for the initially optimized active site ge-

[b] The central axis is defined to be that axis which passes through C_f and which makes equal angles with all three C_f-substituent bond vectors.
[c] A puckering angle of $\theta = 90°$ corresponds to a planar configuration about C_f; 109.4° to a tetrahedral one.
[d] The rotations with respect to the x-ray structure are 17° and 5°, respectively. When viewed along the rotation axis (i.e., from C^γ or C^α to C^β) a counter-clockwise rotation of the imidazole corresponds to a positive rotation angle.

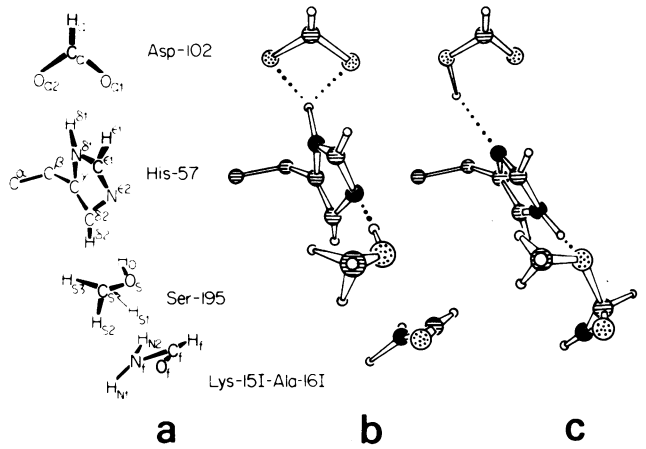

FIG. 1. (a) Symbols used for atoms; (b) atomic positions for initially optimized geometry ($\beta = 0$) and (c) tetrahedral intermediate ($\beta = 1$) with protons transferred. Dotted lines represent hydrogen bonds. Note that C^{α} and C^{β} of His-57 are shown here as reference points for orientation changes in imidazole even though they are not explicitly included in the calculations.

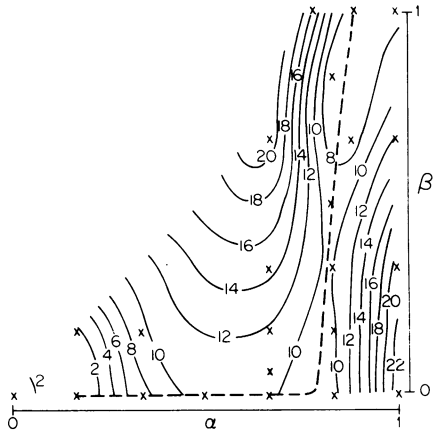

FIG. 2. Potential energy surface of model enzyme system drawn with CONTUR program (ref. 24). ×'s mark calculated energies and dashed line represents the optimal reaction path. All energies are in kcal/mole.

ometry described above. Table 2 demonstrates the charge transfer which accompanies the proton transfer. The imidazole ring appears to gain some negative charge initially, but the principal result is that the methoxy group becomes a powerful nucleophile as α approaches unity.

For the nucleophilic attack by methoxide on formamide a simple rotation of O_s about the C_s–H_{s1} bond axis subsequent to the proton transfer was found to bring O_s uncomfortably close to O_f. However, this problem is resolved if this rotation of 30° is combined with a net lateral translation of methoxide towards C_f by 0.57 Å along an axis parallel to the C_f–O_f bond vector.[e] The formation of the tetrahedral intermediate then proceeds by a translation of formamide towards O_s by 0.63 Å accompanied by a puckering of the carbonyl to θ = 105° and elongations of the C_f–O_f and C_f–N_f bonds to 1.31 and 1.48 Å, respectively. The net result of these motions is to produce a tetrahedral structure (Fig. 1c) which has an O_s–C_f bond distance of 1.56 Å. After formation of the tetrahedral structure, the equilibrium position of neutral imidazole was found to be rotated from its initially optimized orientation by 8.7° and −9.8° about the C^{γ}–C^{β} and C^{α}–C^{β} axes, respectively.[d] This indicates that the imidazole ring, whose mobility has been observed in studies using various acylating agents (5, 11, 13), follows the methoxide as it attacks formamide in order to maintain the hydrogen bond between O_s and the just transferred proton.

The intermediate structures involved here have a very large number of degrees of geometrical freedom, and, thus, it would be prohibitively expensive to vary all of them independently. Therefore, we have chosen to describe the energetics of the reaction path in terms of two judiciously chosen parameters. The first of these is α, the fractional displacement of the two protons from their donor groups to their acceptor groups. The other parameter, β, monitors the several other motions described in the previous paragraph which occur during the nucleophilic attack on the carbonyl carbon of formamide to form the tetrahedral intermediate. We here require that these motions all occur synchronously; i.e., for any structure considered the rotations and displacements included in the β motion are proportional to the fractional progress parameter, β, which ranges from 0 to 1. Our calculated potential energy surface is represented as a contour diagram in Fig. 2, where the optimal[f] reaction path is marked by a dashed line. As noted above, this path does not start at α = 0 and, for similar reasons, does not terminate at α = 1. Physically, this limitation is due to interactions between the residues, such as hydrogen bonding, but MBSE probably exaggerates this effect. The sharp bend in the path at approximately α = 0.8 and β = 0 reflects the apparent nonconcerted nature of this reaction, and indicates that the seryl oxygen will not begin its attack on the peptide linkage until the proton transfer has been nearly completed, at which point the Mulliken charge on the methoxy group has nearly doubled its initial value (Table 2). An important feature of the energy surface is the barrier of some 21 kcal/mole along the diagonal, which prevents the reaction from being completely concerted, i.e., progressing along the line $\alpha = \beta$. The energy profile along the reaction path (Fig. 3) shows that the process is calculated to be slightly endothermic (ΔE = 6 kcal/mole) and to have an energy barrier of 11 kcal/mole. The barrier occurs during the proton transfer phase and may account in part for the deuterium isotope effect observed in acylation (8, 9). The secondary barrier shown in Fig. 3 occurs during the nucleophilic attack but may be an artifact of the restrictions placed on the β motions. Other studies carried out in this laboratory[g] indicate that the linear variation of the several parameters included in β is not completely realistic, and we believe the dashed curve to be more representative of the actual process.

In Table 3 we illustrate the transfer of charge from the methoxy group to formamide, especially O_f, which occurs during the nucleophilic attack on the carbonyl carbon. This attack completes the transfer of negative charge from Asp-102 to the carbonyl oxygen of the scissile peptide linkage in the enzyme mechanism. The formation of a bond between C_f and O_s during this process is accompanied by a weakening of the bonds from C_f to both O_f and N_f, as is reflected by the overlap populations presented in Table 4.

[e] This motion when finally implemented involved a translation of the methoxide anion by 0.33 Å and of formamide in the opposite direction by 0.24 Å. A motion of methoxide by much more than 0.33 Å results in a steric interaction between imidazole and the methyl group of the methoxide ion. Motions of this magnitude should be easily accommodated by the peptide backbone.

[f] Optimal with respect to the projection of the potential energy surface chosen here through the definitions of α and β.

[g] S. Scheiner, D. A. Kleier, and W. N. Lipscomb, manuscript in preparation.

Table 3. Mulliken charges* during methoxide attack

$r_{O_s-C_f}$, Å	Methoxide		Formamide		
	(CH_3)	O_s	O_f	(NH_2)	$(HCONH_2)$
2.82	−0.23	−0.44	−0.20	−0.02	−0.02
2.61	−0.22	−0.43	−0.21	−0.03	−0.05
2.39	−0.20	−0.41	−0.23	−0.05	−0.10
2.18	−0.17	−0.37	−0.28	−0.08	−0.20
1.97	−0.15	−0.33	−0.36	−0.12	−0.35
1.76	−0.09	−0.27	−0.43	−0.15	−0.46
1.56	−0.04	−0.24	−0.51	−0.19	−0.59

* Ref. 23.

In order to better assess the MBSE for the charge transfer in our model enzyme, we studied the transfer of a proton from H_2O to OH^- through the intermediacy of NH_3. The transfer was constrained to pass through a symmetric (C_{2v}) transition state involving a simultaneous transfer of one proton from H_2O to NH_3 and another proton from NH_3 to OH^-. The plot of PRDDO energy versus α (fraction of the full 0.8 Å proton displacements) revealed the energetics of proton transfer in the H_2O–NH_3–OH^- system to be quite similar to those of the transfer in our model enzyme. Both curves have minima at a slight distance from either end point separated by an energy barrier. The 4-31G energy curve for the H_2O–NH_3–OH^- system exhibits minima closer to the end points and an energy barrier of 20 kcal/mole, which is some 10–15 kcal/mole larger than that of the PRDDO curve. We expect a similar correction for our model enzyme system and thus predict that an extended basis set treatment would yield an energy barrier between 20 and 25 kcal/mole if the path in Fig. 2 were followed. Comparison of PRDDO and 4-31G results for the transfer of a proton between methanol and ammonia (a proton displacement of 0.7 Å) and between formic acid and ammonia (1.0 Å displacement) indicate that the MBSE is slightly greater for $[HCOO^- + NH_4^+]$ than for $[CH_3O^- + NH_4^+]$. This suggests that 4-31G calculations would yield a slightly more positive ΔE for the overall reaction than does PRDDO.

DISCUSSION

In this study, the structure of an enzyme–inhibitor complex was used as a starting point for the study of the action of a serine proteinase upon a substrate. Just as with a real substrate, an inhibitor such as PTI is believed to first bind to the enzyme to form a noncovalent complex placing the peptide linkage to be attacked at the active site. The subsequent formation of a tetrahedral intermediate may occur for either the substrate or inhibitor; however, it is hypothesized that either the intermediate does not progress to products in the enzyme–inhibitor complex, or, if it does, that the leaving group–enzyme interaction is too strong to allow a breakup to the acyl enzyme plus amine. In either case the binding of PTI apparently follows the same steps as would productive binding up through the formation of the tetrahedral intermediate. Thus, the use of the trypsin–PTI complex as a starting point for this study should be appropriate.

Table 4. Overlap populations during methoxide attack

$r_{O_s-C_f}$, Å	Mulliken overlap populations* over atoms		
	O_s-C_f	C_f-O_f	C_f-N_f
2.82	0.009	0.854	0.734
2.61	0.022	0.837	0.726
2.39	0.047	0.817	0.713
2.18	0.091	0.790	0.693
1.97	0.155	0.757	0.665
1.76	0.232	0.714	0.636
1.56	0.339	0.662	0.598

* Ref. 23.

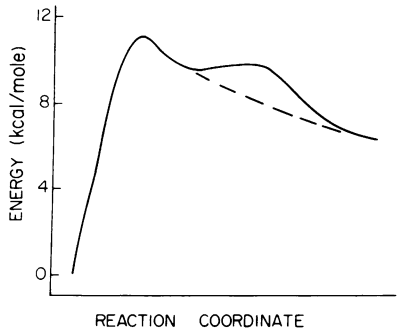

FIG. 3. Energy profile along the reaction coordinate which is defined as the reaction path length of Fig. 2. Dashed line represents that hypothesized for independent variation of parameters included in β.

The placement of the protons in the initial geometry is consistent with the charge state expected at pH > 7 from relative pKa's and is also consistent with geometries obtained through x-ray diffraction studies (5, 10–13). Studies of model systems designed to imitate serine esterase activity have demonstrated the importance of a carboxylate anion for catalysis (18, 19). There is still a controversy, however, over the role of Asp-102 in the charge relay system. Does it remain negatively charged and simply stabilize the positive charge developed on imidazole during the reaction or is it the ultimate proton acceptor in the charge relay? Hunkapiller *et al.* (20) have provided ^{13}C nuclear magnetic resonance evidence that in α-lytic protease the pKa's of the histidine and aspartic-acid residues of interest are 4 and 6.7, respectively. Thus, between pH 4 and 6.7 (or after formation of the tetrahedral intermediate), these two residues should exist as two electronically neutral species rather than as a highly unstable cation–anion ion pair. A structure analysis done in the slightly acid pH range shows an interaction between a *neutral* Asp-102 and His-57 rather than a pair of charged residues (13). In addition, the observation that His-57 is not positioned for the formation of a bifurcated hydrogen bond with Asp-102 at pH 4.5 (11) provides supporting evidence for the conclusion that the residues are neutral at this pH.

Table 1 provides calculated and experimental proton affinities which should be pertinent to the question of proton placement in the His-Asp system after formation of the tetrahedral intermediate. Even though the PRDDO method overestimates experimentally observed proton affinities for similar nitrogenous bases (e.g., ammonia and pyridine), the method still predicts imidazole to have a proton affinity less than that observed (or calculated) for formate anion. Since the environment of the Asp-102 residue is hydrophobic in the enzyme–PTI complex and presumably in an enzyme–substrate complex, these calculations support the contention that Asp-102 acts as the ultimate proton acceptor in the charge relay system. That imidazole is predicted to be a much weaker base than formate anion in the gas phase or in an aprotic medium is not surprising even though this reverses the basicity observed in aqueous solution (21). This conclusion is further supported by evidence that imidazole is not protonated by acetic acid in dioxane unless 1–2 molar equivalents or more of water are present (20).

Since the gas phase proton affinities of methoxide anion and formate differ by 50–70 kcal/mole (Table 1), a direct proton transfer from CH_3OH to $HCOO^-$ or from Ser-OH to Asp^- would probably require a high activation energy. Evidently, imidazole (His-57) greatly facilitates the proton transfer by delocalizing the negative charge (Table 2) and providing stabilizing hydrogen bond interactions preferentially for the transition and final states. The tetrahedral intermediate is stabilized by additional factors which could not be included explicitly in our calculations. For example, the carbonyl oxygen atom which acquires the formal negative charge in the tetrahedral intermediate can form strengthened hydrogen bonds to the N–H groups of Gly-193 and Ser-195 (12). A correction for this stabilization would reduce our calculated ΔE of about 6 kcal/mole to a more thermoneutral value. Further study also revealed that allowing N_f, as well as C_f, to pucker as the tetrahedral intermediate is formed would reduce the calculated ΔE to zero. Our calculated energy barrier after correction for MBSE is 20–25 kcal/mole. This may be compared with the experimental enthalpy of activation of 11 kcal/mole which has been obtained for acylation of a specific ester substrate by chymotrypsin (22). Since the rate-determining step in acylation of esters is formation of the tetrahedral intermediate, the two results should be comparable.

It has been proposed (12) that the breakdown of the tetrahedral intermediate occurs by reversing the charge transfer so that a proton is donated by the His-Asp system to the nitrogen of the scissile peptide linkage. The $C-{+}NH_2R$ bond is then broken and the departure of the neutral amine leaves behind an ester linkage between enzyme and substrate. A preliminary set of calculations indicates that the step is moderately exothermic with an activation energy of 25–32 kcal/mole. The deacylation is hypothesized to be quite similar to the acylation mechanism described above except that a water molecule takes the place of Ser-195 as the nucleophile (1). We plan to report on these latter steps in a future publication.

In summary, our calculations support the following detailed mechanism for formation of a tetrahedral intermediate in amide hydrolysis catalyzed by serine proteinase. The enzyme must be folded to keep solvent out of the region near Asp-102 and this appears to be a crucial function. The aspartate is necessary as the ultimate proton acceptor in the charge transfer which activates the serine nucleophile. Protonation of aspartate at pH $< \sim 7$ thus destroys activity. His-57 serves as a proton relay between the aspartate and serine and also shields Asp-102 from solvent. The freedom enjoyed by the imidazole ring of His-57 due to rotations about the C^α–C^β and C^β–C^γ bonds enables it to easily pick up a proton from Ser-195 and deliver one to Asp-102. However, His-57 is not a passive relay station, since it also serves to delocalize charge during proton transfer and thus facilitate reaction.

A prediction of the dynamics of serine proteinase activity is well beyond the scope of this paper. What we provide is an analysis of an energetically plausible pathway for the formation of a tetrahedral intermediate. In emphasizing energetics here, we have not properly taken into account other effects which promote enzyme activities, such as desolvation and other entropy-related processes.

Note Added in Proof. If $H^{\delta 1}$ is transferred to O_{a1} rather than O_{a2} during the formation of the tetrahedral intermediate, the ΔE for the reaction is unchanged but the activation energy is increased by about 5 kcal/mole. In the optimized final geometry resulting from a transfer to O_{a1}, the imidazole ring lies 10° closer to its orientation in the x-ray structure than it does in Fig. 1c.

We are most grateful to R. Huber for the atomic coordinates which were used as a starting point for this study. We acknowledge Dr. Thomas A. Halgren for his useful comments and assistance with the computations. We thank the National Institutes of Health, Grant GM 06920 for support of this research. We also thank the Office of Naval Research. S.S. thanks the National Science Foundation for a predoctoral fellowship and D.A.K. thanks the American Cancer Society for a Postdoctoral fellowship.

1. Bender, M. L. & Kilheffer, J. V. (1973) *CRC Crit. Rev. Biochem.* **1**, 149–199, and references therein.
2. Bender, M. L. & Thomas, R. J. (1961) *J. Am. Chem. Soc.* **83**, 4189–4193.
3. Fraenkel, G. & Watson, D. (1975) *J. Am. Chem. Soc.* **97**, 231–232. Other recent references are listed here.
4. Caplow, M. (1969) *J. Am. Chem. Soc.* **91**, 3639–3645.
5. Rühlmann, A., Kukla, D., Schwager, P., Bartels, K. & Huber, R. (1973) *J. Mol. Biol.* **77**, 417–436.
6. Zerner, B. & Bender, M. L. (1964) *J. Am. Chem. Soc.* **86**, 3669–3674.
7. O'Leary, M. H. & Kluetz, M.D. (1970) *J. Am. Chem. Soc.* **92**, 6089–6090.
8. Inagami, T., Patchornik, A. & York, S. S. (1969) *J. Biochem. (Tokyo)* **65**, 809–819.
9. Bundy, H. F. & Moore, C. L. (1966) *Biochemistry* **5**, 808–811.
10. Blow, D. M., Birktoft, J. J. & Hartley, B. S. (1969) *Nature* **221**, 337–340.
11. Birktoft, J. J. & Blow, D. M. (1972) *J. Mol. Biol.* **68**, 187–240, and references therein.
12. Huber, R., Kukla, D., Steigemann, W., Deisenhofer, J. & Jones, T. A. (1973) in *Bayer Symposium V, Proteinase Inhibitors*, eds. Fritz, H., Tschesche, H., Greene, L. J. & Truscheit, E. (Springer Verlag, Heidelberg), in press.
13. Krieger, M., Kay, L. M. & Stroud, R. M. (1974) *J. Mol. Biol.* **83**, 209–230.
14. Drenth, J., Swen, H. M., Hoogenstraaten, W. & Sluyterman, L. A. Ae. (1975) *Proc. K. Ned. Akad. Wet. Ser. C* **78**, 104–110.
15. Halgren, T. A. & Lipscomb, W. N. (1973) *J. Chem. Phys.* **58**, 1569–1591.
16. Umeyama, H., Imamura, A., Nagata, C. & Hanano, M. (1973) *J. Theor. Biol.* **41**, 485–502.
17. Lehmann, M. S., Koetzle, T. F. & Hamilton, W. C. (1972) *Int. J. Pept. Protein Res.* **4**, 229–235.
18. Wallerberg, G., Boger, J. & Haake, P. (1971) *J. Am. Chem. Soc.* **93**, 4938–4939.
19. Menger, F. M. & Vitale, A. C. (1973) *J. Am. Chem. Soc.* **95**, 4931–4934.
20. Hunkapiller, M. W., Smallcombe, S. H., Whitaker, D. R. & Richards, J. H. (1973) *Biochemistry* **12**, 4732–4743.
21. Yamdagni, R. & Kebarle, P. (1975) *J. Am. Chem. Soc.* **95**, 4050–4052.
22. Rajender, S., Han, M. & Lumry, R. (1970) *J. Am. Chem. Soc.* **92**, 1378–1385.
23. Mulliken, R. S. (1955) *J. Chem. Phys.* **23**, 1833–1840.
24. Gammill, R. (1974) in *Applications Program Series, AP-38, revision 3* (Massachusetts Institute of Technology Information Processing Center).
25. Ditchfield, R., Hehre, W. J. & Pople, J. A. (1971) *J. Chem. Phys.* **54**, 724–728.
26. Weast, R. C., ed. (1974) in *CRC Handb. Chem. Phys.* (Chemical Rubber Publishing Co., Cleveland, Ohio), p. F-214, E-67.
27. Hanley, M. A. & Franklin, J. L. (1969) *J. Phys. Chem.* **73**, 4328–4331.
28. Taagepera, M., Henderson, W. G., Brownlee, R. T. C., Beauchamp, J. L., Holtz, D. & Taft, R. W. (1972) *J. Am. Chem. Soc.* **94**, 1369–1370.
29. Bak, B., Hansen-Nygaard, L. & Rastrup-Andersen, J. (1958) *J. Mol. Spectros.* **2**, 361–368.